Science of the Total Environment 874 (2023) 162417

Contents lists available at ScienceDirect

Science of the Total Environment

journal homepage: www.elsevier.com/locate/scitotenv

Unmanaged vegetated roofs hydrological performance in subtropical areas: An investigation in São Paulo, Brazil

Lucas Gobatti [a,b,*], Brenda Chaves Coelho Leite [a]

[a] Department of Civil Engineering Construction, Polytechnic School of the University of São Paulo, Prof. Almeida Prado Ave., 83 Jardim Universidade Pinheiros, São Paulo, SP 05508-070, Brazil
[b] Swiss Federal Institute of Aquatic Science & Technology (EAWAG), ETH Zürich, Überlandstrasse 133, 8600 Dübendorf, ZH, Switzerland

HIGHLIGHTS

- In unmanaged vegetated roofs, soil moisture has weak correlation to substrate depth.
- Slow-steady antecedent rainfall decreases roof retention more than intense rainfall.
- Shallow subtropical vegetated roofs have substantial rainwater retention capacities.
- Subtropical summer peak runoffs were considerably attenuated and delayed.
- Unmanaged vegetated roofs are a cost-effective roof alternative for subtropics.

GRAPHICAL ABSTRACT

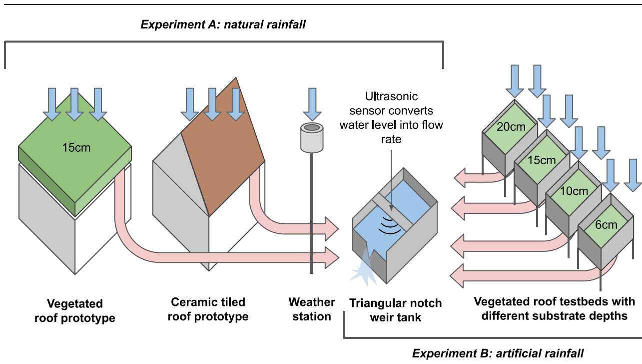

ARTICLE INFO

Editor: Ashantha Goonetilleke

Keywords:
Vegetated roofs
Runoff
Substrate depth
Spontaneous vegetation
Subtropical
Moisture

ABSTRACT

Extensive vegetated roofs are Nature-based Solution with the ability to manage rainwater runoff in densely built spaces. Despite the large amount of research demonstrating its water management abilities, its performance is poorly quantified under subtropical climates and when using unmanaged vegetation. The present work aims at characterizing the runoff retention and detention of vegetated roofs under the climate of São Paulo, Brazil, accepting the growth of spontaneous species. By using real scale prototypes under natural rain, a vegetated roof hydrological performance was compared with a ceramic tiled roof. By using models with different substrate depths under artificial rain, changes in the hydrological performance were monitored for different antecedent soil moisture contents. Results from the prototypes showed that the (*i*) extensive roof attenuated from 30 % up to 100 % the peak rainfall runoff; (*ii*) delayed the peak runoff from 14 up to 37 min and (*iii*) retained from 34 % up to 100 % the total rainfall. Furthermore, results from the testbeds indicated that (*iv*) when comparing two rainfalls with same depths, the one with longer duration can saturate more the vegetated roof and thus undermine more its ability to retain water; and (*v*) when not managing the vegetation, the vegetated roof's soil moisture content loses correlation with the substrate depth, as plants will also develop more and will more effectively restore the substrate retention capacity. Conclusions point to extensive vegetated roofs as a relevant sustainable drainage system in subtropical areas, but demonstrate that its performance is highly dependent on structural factors, weather factors and level of maintenance. Such findings are expected to be useful for practitioners dimensioning these roofs as well as for policy makers towards a more accurate standardization of vegetated roofs in subtropical regions and Latin American developing countries.

* Corresponding author.
E-mail addresses: lucas.gobatti@eawag.ch (L. Gobatti), bcleite@usp.br (B.C.C. Leite).

http://dx.doi.org/10.1016/j.scitotenv.2023.162417
Received 18 November 2022; Received in revised form 24 January 2023; Accepted 19 February 2023
Available online 1 March 2023

1. Introduction

Tropical and subtropical cities tend to go through a considerable amount of intense rainfall events along any given typical year (Vörösmarty et al., 2013), especially during summer (Stevaux et al., 2009). These intense rainfall events become an even greater problem given the way cities are currently built and due to recent accelerated urbanization (Deng et al., 2009). Mainstream urban planning covers up most of pervious areas, turning basins into more and more impervious surfaces (Jacobson, 2011; Shuster et al., 2007), preventing infiltration and evapotranspiration (Wang et al., 2022).

This form of occupying and using the natural surface exceedingly changes the hydrological cycle (Baptista et al., 2011). As a result of impervious soil coverage, surface runoff increases and reaches floodplains in less time (Han and Burian, 2009). These events tend to become hazardous as floodplains are occupied by humans, turning flood risk management a rising concern in a warming climate (Miguez et al., 2015).

In this sense, finding ways of better managing rainwater runoff is imperative and decentralization can be a possibility (Dierkes et al., 2015). Towards this direction, Nature-based Solutions (NbS) are a pathway to be followed, as they can generate a range of Regulatory Ecosystem Services (RES) (Krauze and Wagner, 2019). Among these, as pressure and competition on ground level land use is commonly high in densely populated cities, vegetated roofs (in this article called "VR") stand out (Vesuviano and Stovin, 2013). Roof areas can represent in compact built urban areas up to 50 % of impervious surface (Dunnett and Kingsbury, 2014; Vesuviano and Stovin, 2013).

VR are a type of Nature-based Solution that can locally manage rainfall, retaining a portion of rainfall, delaying and attenuating its peak runoff (Stovin, 2010; Johannessen et al., 2018). These are RES of water regulation, showing these structures' ability to capture water at the point where it precipitates. VR, or green roofs, can not only provide water quantity regulation, but also water quality (Berndtsson, 2010), among many other Ecosystem Services (ES) (Oberndorfer et al., 2007; Shafique et al., 2018).

To evaluate this hydrological performance of a VR, a water budget can be performed. The VR is seen as a water vessel, in which rainfall inflows and can be stored in one of three volumes. First, the unavailable water zone, which is comprised of hygroscopic water closely bound to the soil particles, not useful for plants (Péné et al., 2021; Demirkesen, 2001). Second, the plant available water (PAW) zone, which is comprised of hygroscopic and capillary water. The capillary water is able to move by capillarity through the substrate pores (Demirkesen, 2001). This volume is gradually lost by plant evapotranspiration. The rate by which plants remove water from the substrate is highly influenced by local solar radiation, air temperature and humidity (Getter et al., 2009; Ferrans et al., 2018; Garofalo et al., 2016). The moisture content is somewhere inside the PAW boundaries. It is relevant to note that the higher the initial moisture volume, the lower relative retention will be possible (Liu et al., 2021). And finally, third, the runoff volume, happening when soil field capacity is reached and excess gravitational water starts forming (Péné et al., 2021; Demirkesen, 2001). After this point, soil saturation is reached and runoff begins.

Furthermore, if a rainfall event is sufficiently intense, the soil infiltration rate capacity may be surpassed, generating superficial puddling. This volume of water temporarily stored on the VR surface can be trapped within the roof freeboard framing. After reaching the top of the frame, it becomes overflow. The overflow is particularly relevant for higher slope VRs, where if the infiltration capacity is too low it can lose water for overflow and have the same performance of a regular tiled roof. Illustrations of the concepts presented in this introduction are available in the supplementary materials of this work.

Influencing the VR hydrological performance there are both structural factors and roof conditions at the moment of the rainfall event. As main structural factors, as demonstrated by Liu et al. (2019), the substrate material, its depth, the vegetation choice and the roof slope are relevant factors for the general roof stormwater management performance. But the roof conditions are also relevant, especially regarding water moisture content (Liu et al., 2019; Peng et al., 2019; Voyde et al., 2010).

The vegetation and surrounding environmental conditions count when understanding the soil moisture content dynamics (Poë et al., 2015). As pointed out by Voyde et al. (2010), the evapotranspiration (ET) accounts for 20 % to 48 % of moisture lost. Poë et al. (2015) describe the ET process of water capture, in which plant's roots collect PAW (see Fig. 2) and release it through the xylem towards the leaves' stomatal cavities, which will thus release it to the atmosphere.

Recent studies in tropical and subtropical regions of Brazil are scarce and mainly use small scale laboratory models and adopt succulent or grass plants in their research, but demonstrate a relevant capacity of VR water management in this geographical region (Gobatti and Leite, 2022). Arboit et al. (2021) used small scale models to evaluate the evapotranspiration and runoff rates in a subtropical climate of Brazil. Results for runoff demonstrate that the species used, *Sedum rupestre*, did not provide better water retention performances than a roof module without any vegetation. This can possibly have happened because of these plants' succulency and their Crassulacean Acid Metabolism (CAM), which helps them lose less water and thus recharge less the soil retention capacity by consuming less the PAW.

Still regarding research performed in Brazil, Vacari et al. (2019) analyzed small scale VR models with grass vegetation coverage, shrubs and a mixture of both. Results demonstrated no statistically significant differences from vegetation compositions, but a significant retention rate for all of them. The authors indicate that substrate composition may play a role in the results. Loiola et al. (2019) analyzed modular tray VR systems towards their hydrological performance using succulent plants. The work demonstrates a relevant peak runoff delay and a hydrograph abatement for the VR modular system. Castro et al. (2020) evaluated water quantity and quality performance of VR models in the south of Brazil. Runoff measurements were conducted in low time resolution, only every 3 h, and demonstrated high retention rates in the VR models, ranging from above 50 %.

Wild plants can colonize VRs (Dunnett et al., 2008; Deng and Jim, 2017), and this spontaneous colonization can create interesting opportunities (Vanstockem et al., 2019). Previous works investigated unmanaged VRs and the growth of spontaneous species, pointing out the role of these roofs in generating habitat for species in sealed urban surfaces. Madre et al. (2014) investigated 115 roofs, finding 176 colonizing species, noticing that the functional composition of these communities is shaped among other factors by substrate depth. Catalano et al. (2016) investigated VRs in Germany for 30 years, observed that the planted species gradually gave way to ruderal and more stress-tolerant locally adapted species, concluding that spontaneous colonization should be considered for more resilient VRs. In the two VRs observed by Thuring and Dunnett (2019), less than half the original planted species persisted over time, but the entirety of the green cover was maintained by colonizing species. (Ouellet et al., 2021) compared managed and unmanaged VR and observed that the unmanaged had a greater capacity in reducing thermal surges associated with storm events. Not only that, but Schrieke and Farrell (2021) demonstrated spontaneous VRs can reduce construction costs, applying less pressure on property value.

Previous work showed that unmanaged VRs can favor the wellbeing of citizens as well as serve the conservation of urban biodiversity (Aloisio et al., 2020). Schrieke and Farrell (2021) argue that spontaneous species may also contribute to stormwater retention in VRs given that some of them have 'fast' traits such as fast growth or higher leaf area and high transpiration assisting on the replenishment of substrate storage capacity. Spontaneous species can also establish on VRs without irrigation or fertilizers, being able to colonize even the shallowest substrates (Schrieke and Farrell, 2021). However, no work has been found evaluating the hydrological performance of such roofs, especially given different substrate depths and in subtropical climates. The literature indicates that the role of spontaneous vegetation on VR hydrological performance is unclear (Robinson and Lundholm, 2012; Schrieke and Farrell, 2021).

As of environmental influences of subtropical climates, the evapotranspiration rates and rainfall events are the main concerns regarding the water balance in VRs (Poë et al., 2015; Peng et al., 2019). Previous studies show that there has been very little VR water quantity performance investigation under tropical and subtropical climates (Blank et al., 2013; Grullón-Penkova et al., 2020) but it is an increasingly investigated topic (Liu et al., 2021). Geographical differences for the VR performance towards water management are relevant, as pointed out by Poë et al. (2015). Locatelli et al. (2014) show that retention rates are higher in warmer climates if compared to temperate climates, where the bulk of VR studies are concentrated (Blank et al., 2013). Hakimdavar et al. (2014) demonstrate how the higher incidence of storm events also influences water retention, diminishing the VR performance, and the parameters that most influence this phenomenon are rainfall depth and event duration.

There is a need for local analysis, in the sense that it is qualitatively known how VR performs, but quantification in the subtropical areas is yet insufficient. Therefore, the present experimental investigation is undertaken in São Paulo, Brazil. The city is under a transitional zone between tropical and subtropical climates within the country, as the Köppen Geiger climate classification indicates (Alvares et al., 2014). Martinelli (2010) classifies São Paulo as a Cwa (Humid subtropical zone, with dry winter and hot summer) on larger scale referencing maps, in close transition to Aw (Tropical zone, with dry winter).

The subtropical climate conditions and the use of unmanaged vegetation influences on the VR hydrological performance are the main research gaps investigated in the present research. We monitored laboratory built real scale VR and VR testbeds to compare the rainfall-runoff, generating hydrological data for unmanaged VR in the subtropical Brazil. The main novelty found by our work lies on the influence this vegetation has in the hydrological performance of VR in subtropical climates, given different substrate depths and given the particularities of rainfall events in this climate region. The use of native and spontaneous species on VR structures can have a beneficial effect on restoring the substrate capacity to better retain stormwater due to its local adaptability and is therefore relevant to be investigated.

South America is home for developing countries which are yet standardizing the use of Nature-based Solutions (Castillo and Crisman, 2019). Therefore, results are relevant in order to support the correct design and planning towards mainstreaming these structures. Extensive, lightweight and unmanaged VR are a possibility for decentralizing water management, as they are less demanding for the building structures, making it possible to install them in un-retrofitted buildings (Silva et al., 2017). If unmanaged roofs can yet generate relevant water retention and detention in a subtropical area, this can be a way forward towards sustainable drainage.

To address this hypothesis, the main objectives of this work are to (*i*) quantify the extensive VR retention and detention performances in terms of rainwater capture, peak runoff delay and peak runoff attenuation under the subtropical area of São Paulo. And to further expand the results, the work also aims at (*ii*) demonstrating how unmanaged vegetation and the specifics of subtropical climate conditions can influence the retention and detention performances of VR.

2. Materials and methods

In order to reach the characterization of the hydrological performance of extensive VRs, two complementary experiments are set up. The first, experiment A, compares the rainfall-runoff of two masonry building prototypes, one with a VR and another with a commonly used ceramic tiled roof, both under natural rain. The second, experiment B, compares the rainfall-runoff of four testbeds with varying VR substrate depths using simulated rainfall. The complete experimental setup is illustrated and photographed in the supplementary files.

2.1. Runoff data capture

For both experiments, a common phenomenon to be characterized is the roofs' runoff, which is flow rate based. As indicated by Naveen et al. (2020), regular commercial flowmeters tend to be expensive or only able to read in specific conditions. Arduino-based flow rate sensors, though inexpensive, may also not provide the adequate precision for such a small discharge. To address this issue, a triangular notch thin plate tank was attached to each prototype and testbed outlet in order to accurately capture the runoff. The setup is here described in general lines, but can be found in more detail at Gobatti et al. (2022). This weir can be used for measuring small flow rates ($q < 30l/s$) and is, thus, adequate for the proposed application.

Attaching this weir to a tank and measuring its water level can generate sufficiently accurate flow rate estimations (El Hattab et al., 2018). Based on Eq. (1), as in Shen (1981) and El Hattab et al. (2018), if the water level is above the weir notch vertex the rate of pouring water is:

$$q = \left(\frac{8}{15} \times 0.61\right)\sqrt{2g}\,\tan\left(\frac{\theta}{2}\right)h^{5/2}\ \left[\mathrm{m}^3/\mathrm{s}\right] \tag{1}$$

where θ is the triangular notch angle, g the Earth's gravity acceleration, h the water level measured from the weir notch vertex, as seen in Fig. 1.

To infer the flow rate for any water level (L) in the weir tank, Eq. 2 is used. In these equations, t is the time, i is a generic timestep counter, A and B are the tank dimensions, T is the time of a timestep i in seconds, and Q_{runoff} is the final flow rate:

$$Q_{runoff,t=i} = \begin{cases} \left[(L_{t=i} - L_{t=i-1}) \times A \times B\right]/T\ \left[m^3/s\right], 0 < L \leq P \\ q_{t=i}\ \left[m^3/s\right], P < L < P + h_{max} \end{cases} \tag{2}$$

Fig. 1 shows the US-025 ultrasonic sensor positioning, which should be parallel to the water level (Nair et al., 2019). The ultrasonic sensor sends a trigger sound pulse and measures the time taken until the pulse echoes back, inferring the distance by the speed of sound as seen in Panda et al. (2016). A kinetic dumping barrier made of loose stone is added to diminish the surface waves from the runoff mechanical energy.

Finally, in order to find the total rainfall volume during a given event, Eq. (3) is used, presented in its continuous and discrete forms:

$$Q_{runoff} = \int_0^t Q_{runoff,t=i}dt\ \left[m^3\right]\ or\ \sum_i\left(Q_{runoff,t=i} \times T\right)\ \left[m^3\right] \tag{3}$$

2.2. Rational method

The Rational Method was used in order to characterize rainfall retention rate for each VR event. As Loiola et al. (2019) point out, it is a method classically applied to micro-drainage and used in small urban catchment areas, and is demonstrated in Eq. (4).

$$Q = C \times i \times A_{roof} \tag{4}$$

In the equation, Q represents peak hydrograph; i is a design rainfall intensity; A_{roof} the roof area and C is a dimensionless runoff coefficient. This coefficient depends on the catchment surface conditions, use and occupation, varying from zero to one. It tends to zero when surface runoff is low, that is, in permeable surfaces such as forests and parks; and tends to one when surface runoff is high, that is, in impervious surfaces such as asphalt. Thus, Eq. (5) presents C:

$$C = \frac{Q_{runoff}}{R}, C \in [0, 1[\tag{5}$$

where R is the total rainfall (m^3). To use a more intuitive coefficient, the present work adopts RR as the complimentary coefficient to C, representing the retention rate. RR (Eq. (6)) represents the proportion of the total rainfall retained by a VR, varying from zero to one:

$$RR = \frac{R - Q_{runoff}}{R} = 1 - C, RR \in]0, 1] \tag{6}$$

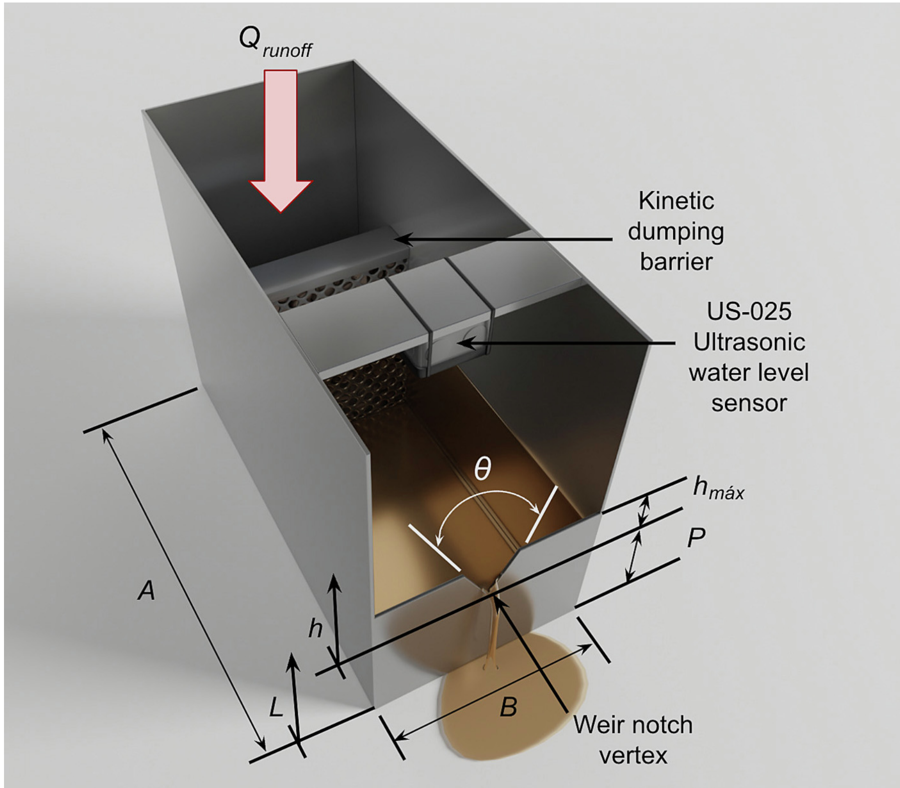

Fig. 1. Triangular notch thin plate weir tank dimensions. Illustrated by Henrique Capanema, adapted by the authors. (For interpretation of the references to color in this figure legend, the reader is referred to the web version of this article.)

2.3. Experiment A

The first experiment characterizes the rainfall-runoff of two prototypes, one with a 15 cm deep extensive VR and another with a CT roof. Both prototypes are 3 m × 3 m, built outdoors using masonry and simulating a real scale building with a door and a window, as seen in Ferraz (2012).

The VR prototype is a ten-year unmanaged and un-irrigated roof. Its vegetation after such time has become dominated by an invasive grass species, turning into a spontaneous but homogeneous culture. As indicated by Dunnett et al. (2008), if totally unmanaged, a roof can become fully controlled by aggressive species that may decrease the roof biodiversity.

Real-time sensing is undertaken for runoff rates using the aforementioned setup, and other sensors also collaborate. Two different pluviometers capture rainfall data, one an *in-situ* Vantage Vue weather station with a 1 min resolution (Davis Instruments, 2021) and another laboratory made pluviometer about 400 m distant with a 5 min resolution. Not all data was available from the *in-situ* station, thus the other close-range pluviometer was used. A HOBO solar radiation sensor S-LIB-M003 (Onset, 2022a) with a H21-USB data logger (Onset, 2022b) collected data regarding sunlight intensity. The S-LIB-M003 is a Silicon Pyranometer with a measurement range of 0 to 1280 W/m^2 over a spectral range of 300 to 1100 nm, with a ± 5 % accuracy.

Five relevant characteristic rainfall events during a summer period from Nov/2021 to Feb/2022 were chosen (Events A1 to A5) from a larger range of collected data, as seen in Fig. 2. These represent different rainfall intensities, durations and time gaps from previous rainfall events. Such parameters illustrate different demands for a VR, as seen in Liu et al. (2019), and thus may generate different relevant performance outcomes. The figure

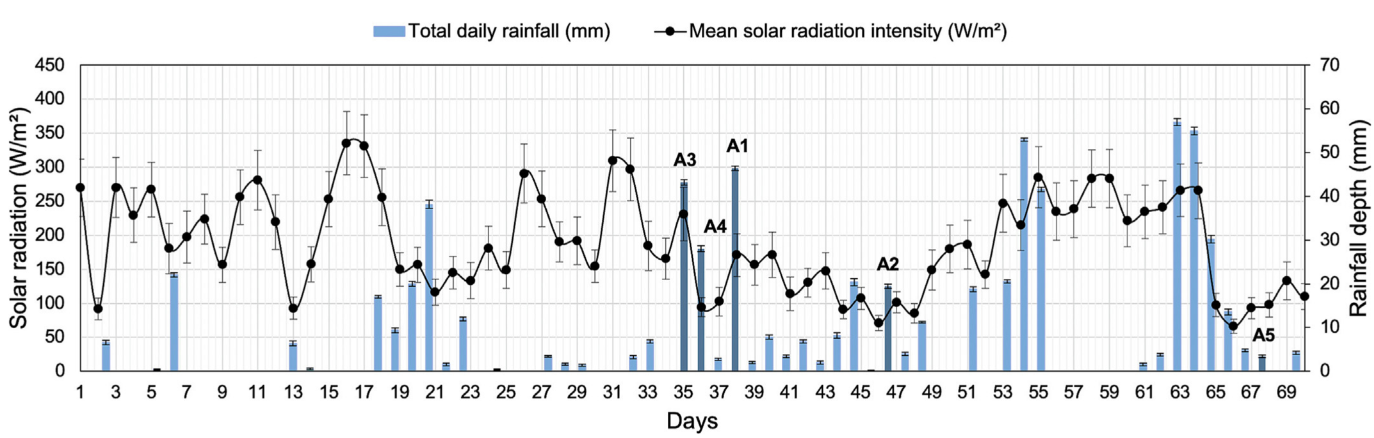

Fig. 2. Rainfall and solar radiation dynamics during the experiment duration, highlighting in darker hatch the events analyzed, Events A1 to A5. (For interpretation of the references to color in this figure legend, the reader is referred to the web version of this article.)

shows both solar radiation dynamics during the event days and previous days as well as total daily rainfall. The events are characterized quantitatively using the intensity-duration-frequency (IDF) equation of São Paulo (DAEE-CTH, 2018) in the supplementary files.

Event A1 is representative of summer evening rainfalls, having the highest intensity of all events analyzed and a short duration. Event A1 has also happened at the end of a sequence of concentrated intense rainfall events. Event A2 is representative of rainfalls that last for many minutes, having all 15 of its previous days seen precipitation. Event A3 is representative of rainfall events right after dry periods, having 12 of its previous days not seen any rain or very little precipitation. Event A4 is representative of events a day after an intense precipitation, as the last rain event happened less than 4 h before. Event A5 is representative of small intensity and long duration events. Events A1, A4 and A5 had two separate peak rainfalls. These events had their peaks analyzed separately.

Knowing the rainfall rate (inflow) and the runoff rate (outflow), an estimate of the VR retention can be made, which is the roof capacity to store water (Stovin, 2010). After this water budget realization, an analysis of the VR detention capacity is undertaken. The detention characterizes the ability of the VR in delaying and decreasing the peak runoff (Stovin, 2010). As it is expected that the retention and detention rates will vary depending on the previous soil moisture conditions Liu et al. (2019), a second experiment under more controlled conditions is built.

2.4. Experiment B

The second experiment has the capacity to characterize runoff for different substrate depths and soil moisture contents. Four 1.4 m × 1.3 m testbeds are built with pine wood and machined aluminum profile structure with varying substrate depths (Model M1 with 20 cm, M2 with 15 cm, M3 with 10 cm and M4 with 6 cm). In order to simulate rainfall events, an irrigation system is installed. The system consists of a Rain Bird controller that can open and close solenoid valves at programmed intervals, the piping system and a set of 15 calibrated drip nozzles for each testbed (Rain Bird, 2003).

Given that in experiment A we were not able to measure soil moisture content, experiment B was designed to also fill in this gap: rainfall events were simulated using the irrigation system, which applied a constantly uniform irrigation homogeneously over the models. This allowed us to measure before and after each rainfall event the soil moisture content using a handheld probe. The same constant irrigation was input at different controlled events (Event B1, Event B2, Event B3) when varying the soil moisture content. This moisture content variation was achieved by letting all testbeds dry out without irrigation, increasing their antecedent dry weather period (ADWP) for each event. Testbeds were left without irrigation for 24 h in Event B1; for 48 h in Event B2 and for 72 h in Event B3.

Soil moisture content data was collected using a Extech MO297 portatile pinless moisture meter and an MO290-EP extension moisture probe with dual sharp 8.5 cm pins (Extech, 2009; Extech, 2014). The sensor can work within a 13 % to 99 % moisture range and provide an accuracy of ±5 %. It is known that for such loose and porous substrates used in VRs the moisture meters can give significant reading variations (Hill et al., 2015). Thus, having many readings is necessary for reaching a mean value closer to the substrate reality. For that, an experiment under controlled conditions where rainfall events can be simulated becomes useful, as one only moisture meter can be used to infer data in a variety of points along the testbed surface before the irrigation starts.

The treatment gave to each testbed was identical: at first a homogeneous plantation of *Arachis repens* is performed in all testbeds and then vegetation in the testbeds is left unmanaged, generating space for spontaneous individuals to grow. It is used between roofs an identical substrate mixture of (in vol.) 64 % mixed organic compost, ashes, crushed and composted pine and eucalyptus bark; 12 % coconut coir fiber dust; 12 % mixed grain sand and 12 % mixed grain vermiculite.

2.5. Data analysis and error

Statistical data analysis was used when necessary and errors related to the methods used were propagated. For experiment A, solar radiation data is represented as its mean intensity and a confidence interval of 95 % around its average. For experiment B, moisture content and irrigation rates were characterized *via* its mean and a standard error. Experiment B tendency lines are a two-period moving average in order to smooth out runoff sensor measurement fluctuations.

Errors are based on nominal instrument uncertainties indicated by the manufacturer or estimated as half the equipment precision. Errors are propagated whenever an arithmetic operation between measurements containing errors is made, based on Tellinghuisen (2001).

For summing up the inflow measurements, if using weather station data or irrigation data, the process is the same. Let R be the sum of each $R_{t=i}$ inflow for each timestep i in an event. The error δR is given in Eq. (7):

$$\delta R = \sqrt{\sum_i \left(\delta R_{t=i}^2\right)}\ [\text{mm}] \tag{7}$$

where $\delta R_{t=i}$ is the measurement error for the inflow at a given timestep i.

For finding the runoff $Q_{runoff,\ t=i}$ (or outflow) error for a given $t = i$ timestep, the error is coupled to the weir tank error. The triangular notch weir tank flow rate error is derived from the error of the variable h, which is δh. Eq. (2) can be written in the form of Eq. (8), where k is constant when varying only h:

$$Q_{runoff,t=i} = k \times h_{t=i}^{5/2}, P < L < P + h_{max} \tag{8}$$

How $Q_{runoff,\ t=i}$ varies for any $h_{t=i}$ variation is answered by partially deriving for h, which yields Eq. (9):

$$\frac{\partial Q_{runoff,t=i}}{\partial h_{t=i}} = \frac{5}{2} \times k \times h_{t=i}^{3/2}, P < L < P + h_{max} \tag{9}$$

Hence, dividing by Q_{runoff}, the error δQ_{runoff} will be the Eq. (10):

$$\delta Q_{runoff,t=i} = Q_{runoff,t=i} \times \left(2.5 \times \frac{\delta h_{t=i}}{h_{t=i}}\right), P < L < P + h_{max} \tag{10}$$

The Eq. (10) indicates that in terms of relative errors, a 1 % error in the water level means a 2.5 % flow rate error for the zone where water is pouring from the weir, or $P < L < P + h_{max}$. This error does not take into account the error of θ. The water level error for the proposed setup is associated with the ultrasonic sensor error and data acquisition frequency, which for the present work yielded $\delta h = 0.2mm$ for any $t = i$.

For the zone where $0 < L \le P$ errors are propagated from an arithmetical multiplication of errors associated with a sum of errors. As L is a function of h, its basic error is the same $\delta L = 0.2\text{mm}$ for any $t = i$. This process is seen in Eq. (11):

$$\delta Q_{runoff,t=i} = Q_{runoff,t=i} \times \sqrt{\left(\frac{\sqrt{\delta L_{t=i}^2 + \delta L_{t=i-1}^2}}{|L_{t=i} - L_{t=i-1}|}\right)^2 + \left(\frac{\delta A}{A}\right)^2 + \left(\frac{\delta B}{B}\right)^2}, 0 < L < P \tag{11}$$

To find the total δQ_{runoff}, the sum of errors propagation is used. Hence, Eq. (12) is used to find the total error for the total runoff volume of a rainfall event:

$$\delta Q_{runoff} = \sqrt{\sum_i \left(\delta Q_{runoff,t=i}^2\right)}, 0 < L < P + h_{max}\ [\text{m}^3/\text{s}] \tag{12}$$

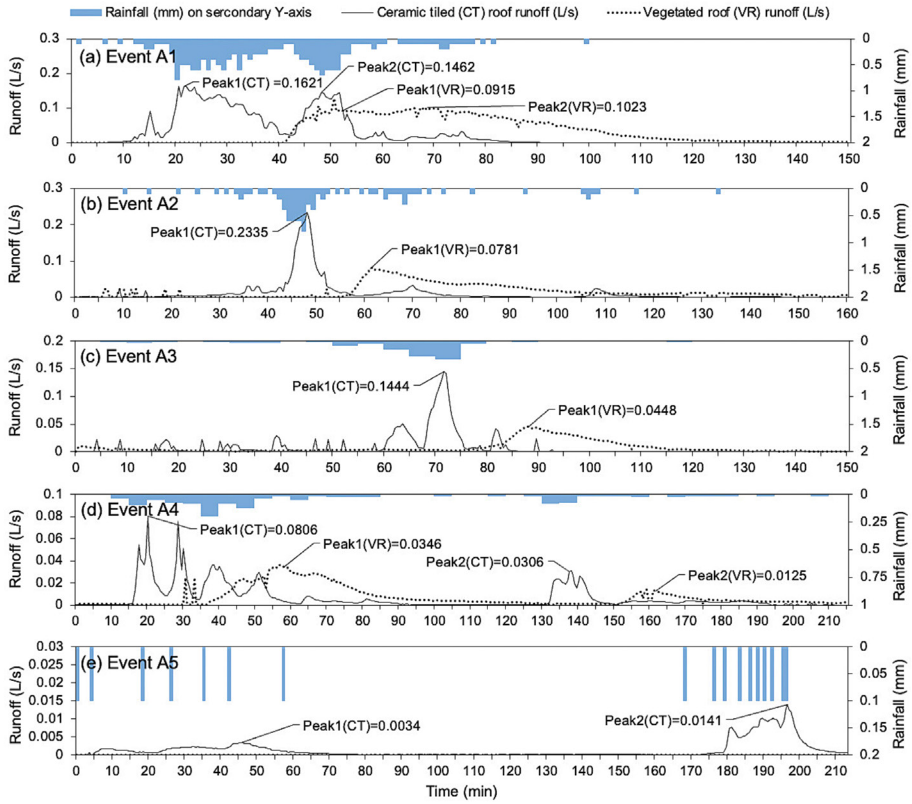

Fig. 3. (a-e) - Rainfall-runoff hydrographs for five characteristic events, A1 to A5. (For interpretation of the references to color in this figure legend, the reader is referred to the web version of this article.)

3. Results and discussion

Each of the two experiments generated specific relevant results. The main findings are separated in two sections, describing patterns observed and applicable correlations for each investigation.

3.1. Experiment A results

Fig. 3 shows the rainfall hydrographs for events A1 to A5 and the runoff for the VR prototype and ceramic tiled (CT) prototype. For all events, it is noticeable that the weather station captures rainfall about the same time the runoff is being captured by the CT weir tank. However, VR runoff delays not only to start, but its peak is also delayed and attenuated.

Table 1 shows a water balance for each event, respectively for the CT and VR prototypes. For all events, the ten-year unmanaged VR was able to retain considerably more rainfall than the CT. In Event A5, the CT proportionally retained a relevant amount of water, but that is because A5 was a very small rainfall depth event, in which the simple soaking of tiles already consumed most of the rainfall. Also, for the same E5, the VR prototype collected 100 % of the rainfall, which shows there are low intensity events that can generate no runoff for VRs.

Besides Event A5, the event in which the proportion retained was higher was A3. A direct indication that an intense event right after a dry period may be where the VR should have a higher performance. This is because most of the water saturating the soil has been removed by ET. The event that retained proportionally less rainwater was A2: a medium intensity event right after many days of rain and a low solar radiation period. The low solar radiation is an indicator of low ET, which is the main mechanism for desaturating the roof. Events A1 and A4 had similar performance, showing that a one-day gap may not be relevant for any major changes in runoff retention.

Table 2 demonstrates a compared detention performance between both CT and VR prototypes. For any event with two peaks (Peak 1 and Peak 2), it is straightforward to notice that the second peak (Peak 2) always has a smaller or equal peak runoff attenuation and delay effect. That is because the VR is already exceedingly saturated. Despite not having the best

Table 1
Retention performance under each rainfall event for CT and VR.

Roof type	Event	Rainfall	Runoff	Retention	RR
		(*L*)	(*L*)	(*L*)	(*1*)
Ceramic tiled roof (CT)	Event A1	511.36 ± 8.08	501.6790 ± 0.0063	9.68 ± 8.08	0.019 ± 0.016
	Event A2	228.48 ± 6.61	227.6452 ± 0.0042	0.84 ± 6.61	0.004 ± 0.029
	Event A3	151.34 ± 8.33	143.1728 ± 0.0025	8.17 ± 8.33	0.054 ± 0.055
	Event A4	172.55 ± 11.78	166.6702 ± 0.0017	5.89 ± 11.78	0.034 ± 0.068
	Event A5	46.24 ± 1.86	36.7002 ± 0.0001	9.54 ± 1.86	0.206 ± 0.041
Vegetated roof (VR)	Event A1	440.01 ± 8.06	289.5352 ± 0.0060	150.47 ± 8.06	0.34 ± 0.19
	Event A2	196.60 ± 6.60	147.6277 ± 0.0030	48.97 ± 6.60	0.25 ± 0.35
	Event A3	130.22 ± 8.33	66.3227 ± 0.0015	63.90 ± 8.33	0.49 ± 0.71
	Event A4	148.48 ± 11.78	91.6693 ± 0.0015	56.81 ± 11.78	0.38 ± 0.09
	Event A5	39.78 ± 3.97	0.0 ± 0.0	39.79 ± 3.97	1.00 ± 0.14

Table 2
Compared detention performance for each rainfall event and peak.

Event	Peak 1			Peak 2		
	Attenuation		Delay	Attenuation		Delay
	(L/s)	(%)	(min)	(L/s)	(%)	(min)
Event A1	0.0705 ± 0.0405	43.5 ± 0.3	30.5 ± 0.5	0.0439 ± 0.0362	30.0 ± 0.3	20.5 ± 0.5
Event A2	0.1554 ± 0.0531	66.6 ± 0.3	14.0 ± 0.5	No peak 2	No peak 2	No peak 2
Event A3	0.0996 ± 0.0311	42.7 ± 0.2	15.0 ± 0.5	No peak 2	No peak 2	No peak 2
Event A4	0.0460 ± 0.0177	57.0 ± 0.2	37.0 ± 0.5	0.0180 ± 0.0064	58.9 ± 0.2	24.0 ± 0.5
Event A5	0.0034 ± 0.0006	100 ± 0.0	–	0.0141 ± 0.0027	100 ± 0.0	–

retention performance, Event A2 was the most attenuated peak, followed by A4 which also did not have the best retention performance. That is because both had smaller rainfall intensities and greater rainfall duration, yielding less water pressure to generate runoff. Greater peak runoff delay was obtained in Event A4 for the same reason.

3.2. Experiment B results

Experiment B results are shown in Fig. 4, for three different events: Event B1, Event B2 and Event B3. Events differ by the antecedent dry weather period (ADWP). The runoff was measured for a steady 0.0325 L/s irrigation income. Here there are results which confirm what is already established in the field, and the next sections will bring results which are novel and can contribute to further understand the hydrological performance of vegetated roofs within subtropical climates and using unmanaged vegetation.

As known in the literature, it is noticeable that on average greater soil depths yields also longer delays for runoff to start and the smaller is the peak runoff reached. It is also noticeable that the shallow 6 cm (Model M4) and 10 cm (Model M3) can overlay or switch positions, indicating what can be a minimum threshold performance. From one event to another, as soil moisture content decreases, the delay for runoff to start increases. The *plateau* all curves reach is not parallel to the X-axis, but is inclined. For a longer experiment, runoff would eventually equal the inlet irrigation when full soil field capacity is reached.

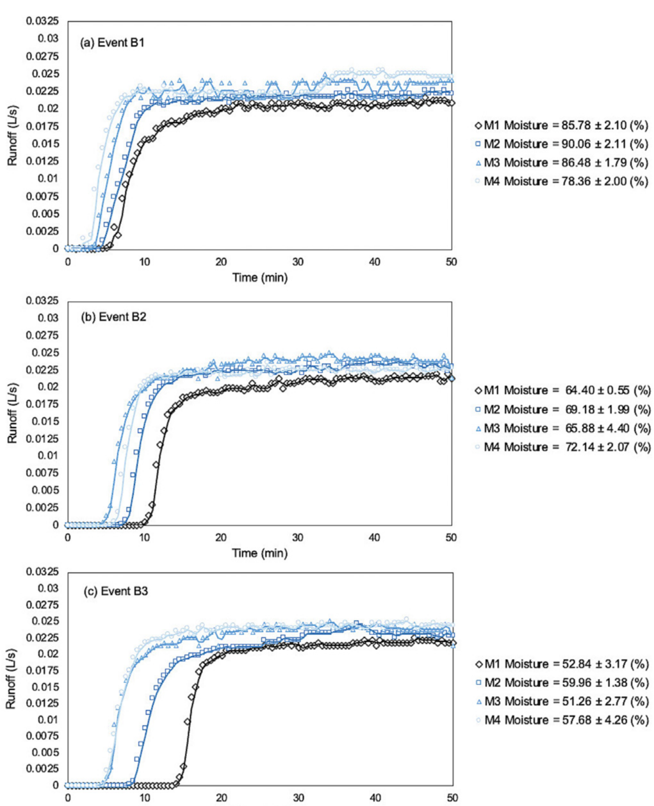

Fig. 4. (a-c) - Runoff obtained for different substrate depths (Models M1 to M4) and different soil moisture contents during controlled simulated rainfall events (Events B1 to B3) with same intensity and duration. (For interpretation of the references to color in this figure legend, the reader is referred to the web version of this article.)

Comparing the detention performance for each event under different soil moisture conditions yields the results on Table 3. The moment when runoff starts is considered to be when flow rate first reaches a 1 mL/s threshold. Each model peak runoff for the imposed irrigation of 0.0325 L/s is calculated as the average runoff between 45 and 50 min, which will increase as the full soil field capacity is reached. In the experiment as a whole, the proportion of total irrigation retained (RR) varied from 0.340 ± 0.005 (Event B1, Model M4) to 0.548 ± 0.006 (Event B3, Model M1), depending on substrate depth and previous moisture content. Runoff starting time was also delayed from 2.5 ± 0.5 min (Event B1, Model M4) all the way to 14.5 ± 0.5 min (Event B3, Model M1).

3.3. Unmanaged vegetation effects

The correlation between initial soil moisture content and substrate depth and the consequences on relative retention and on the time when runoff starts can be seen graphically in Fig. 5.

Positive strong correlations happened between RR and the substrate depth and also to the delay in time runoff. This means that as substrate depth increases, so does rainfall retention and the time for runoff to start, which is corroborated by previous works such as Liu et al. (2019) and VanWoert et al. (2005). Fig. 5 also shows that substrate depth has a greater influence in the retention amount than in the detention delay. An also strong and positive correlation is observed between the proportion retained and the time runoff starts. This means that the more rainfall the substrate retains, the greater is the runoff delay.

On the other hand, there is a negative correlation between antecedent soil moisture content (ASMC) and the proportion retained as well as to the time runoff starts. This indicates that as ASMC increases, the proportion retained decreases, which is in harmony with Liberalesso et al. (2021) and Soulis et al. (2017), but also in harmony with Persch et al. (2021) that shows this correlation is weak. This also indicates that as ASMC increases, the delay for runoff to start decreases, which is physically coherent and coherent with the literature.

However, here lies a relevant effect of the unmanaged and spontaneous vegetation related to substrate depth and soil moisture content. The ASMC wasn't correlated to the substrate depth, which is counterintuitive, as it was expected that the deeper the substrate the more it would be able to retain. This can be explained by the fact of the VRs being unmanaged: higher substrate depths also had greater biomass and thus greater evapotranspiration rates, as also described by Schrieke and Farrell (2021). This is a very interesting novel outcome pointing to the possibility that in unmanaged VRs ASMC loses correlation to substrate depth, also indicating that unmanaged vegetation can be more effective in restoring the substrate retention capacity, which is also supported by Schrieke and Farrell (2021), and that shallow vegetated roofs may be as effective as deeper substrates in terms of soil moisture maintenance in these cases. Deeper substrate depths will indeed retain more moisture, but its unmanaged vegetation will also grow

Table 3
Retention and detention obtained for Events B1, B2 and B3.

Event	Parameter	Model M1 (20 cm)	Model M2 (15 cm)	Model M3 (10 cm)	Model M4 (6 cm)
Event B1	ASMC (%)	85 ± 7	90 ± 7	86 ± 7	78 ± 7
	Delay (min)	6.0 ± 0.5	4.5 ± 0.5	4.0 ± 0.5	2.5 ± 0.5
	Retention (L)	46.44 ± 0.49	40.95 ± 0.49	35.48 ± 0.49	33.15 ± 0.49
	RR (1)	0.476 ± 0.006	0.420 ± 0.005	0.364 ± 0.005	0.340 ± 0.005
Event B2	ASMC (%)	64 ± 7	69 ± 7	66 ± 8	72 ± 7
	Delay (min)	10.5 ± 0.5	8.0 ± 0.5	6.5 ± 0.5	6.5 ± 0.5
	Retention (L)	50.28 ± 0.49	42.08 ± 0.49	41.43 ± 0.49	40.49 ± 0.49
	RR (1)	0.516 ± 0.006	0.432 ± 0.005	0.425 ± 0.005	0.415 ± 0.005
Event B3	ASMC (%)	53 ± 7	60 ± 7	51 ± 7	57 ± 8
	Delay (min)	14.5 ± 0.5	9.0 ± 0.5	5.0 ± 0.5	5.0 ± 0.5
	Retention (L)	53.40 ± 0.49	44.81 ± 0.49	36.46 ± 0.49	34.96 ± 0.49
	RR (1)	0.548 ± 0.006	0.460 ± 0.006	0.374 ± 0.005	0.359 ± 0.005

and proliferate more, creating an increased functional diversity (Cook-Patton and Bauerle, 2012), meaning it will then release more water as ET.

3.4. Subtropical climate effects

Results of experiment A demonstrate that the VR not only captures water within its substrate, but also delays runoff arrival to the urban rainwater drainage system. A conceptual representation of this phenomenon can be seen in the supplementary files. In the experiment B, despite the experimental errors and measurement uncertainties, it is possible to observe that none of the runoff curves presented in Fig. 4 equal the inflow simulated rainfall of 0.0325 L/s. As soil dries out, the capillary water present in the soil is gradually lost. The hygroscopic water represents, thus, a bigger proportion of soil moisture content as this moisture decreases. A less water saturated substrate means a higher air saturated substrate. This signifies that rainwater (or irrigation) has to rebuild the gravitational paths around the soil particles. But this path construction takes time and energy.

This finding gives a relevant insight to previously well-established ASMC correlations like in Tucci (2005). In his work, the author associates soil moisture only with rainfall depth in the previous five days from an event. Soil moisture content, however, may thus be more closely correlated to rainfall intensity and duration in previous days, as this correlation would better account for the time water takes to actually saturate the soil pores. Runoff will increase at different rates, as shallow soil should be easier for water to flow through and deep soil more difficult.

Hence, despite there may be runoff and thus gravitational water, for the full field capacity to be reached it takes time. That is, within the same block of soil (or VR) there can be zones with gravitational water, capillary water

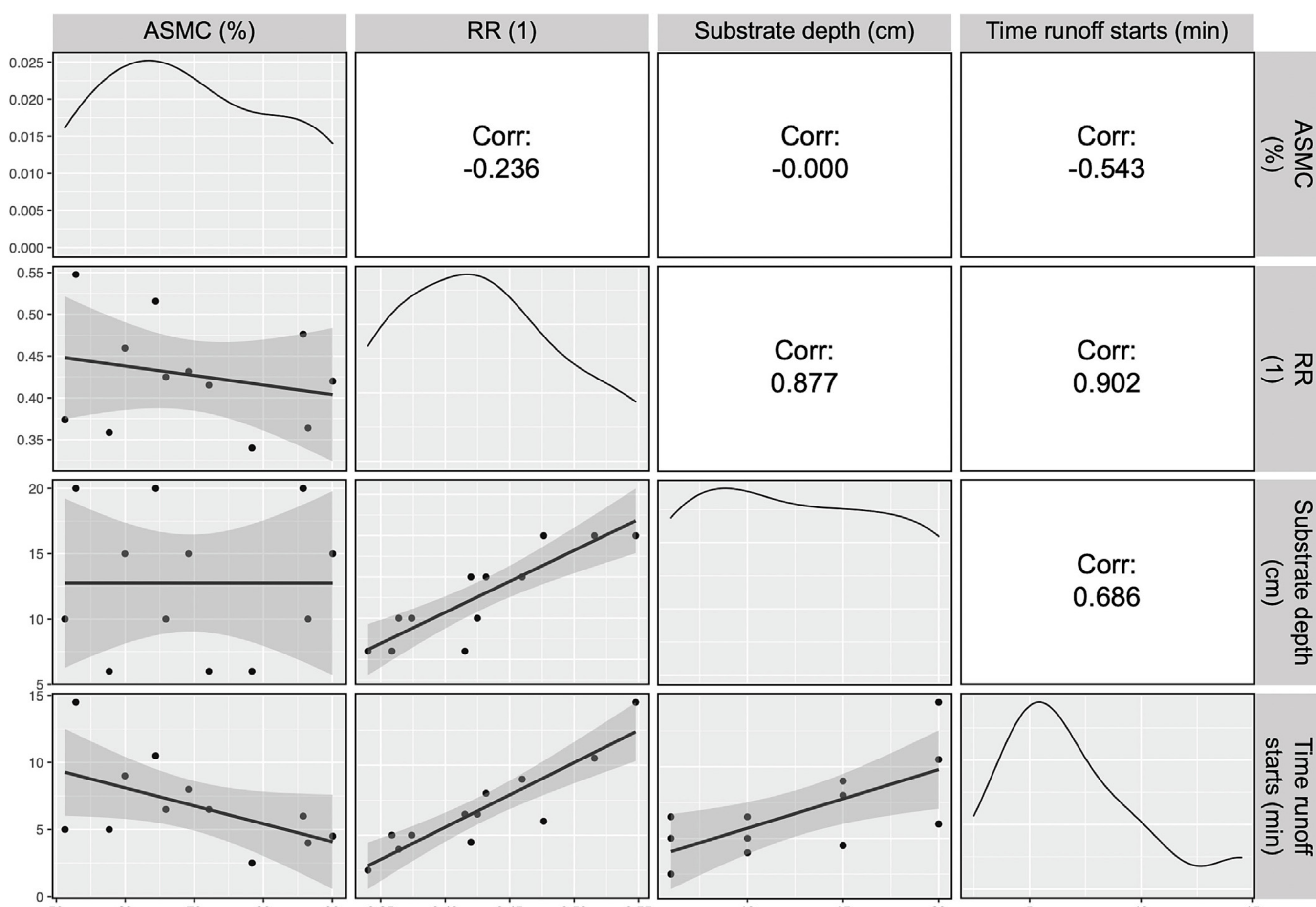

Fig. 5. Correlation matrix for substrate depth, soil moisture content, relative retention and the time runoff starts for a 0.0325 L/s irrigation under experiment B conditions. The highlighted areas represent $p < 0.05$.

and only hygroscopic water simultaneously. Vegetated roofs producing runoff even in unsaturated substrate conditions is in harmony with the literature.

In terms of how different precipitation characteristics influence the hydrological performance of a VR, Experiment B has an interesting outcome. It points to the possibility that a large number of previous days with a slow but steady rainfall intensity can reduce the soil retention capacity more than a short and intense previous day of rain, which explains a lot of the outcomes observed in the Event A2 from experiment A, in comparison to Event A4 from experiment A. As seen in Fig. 2, Event A2 had a steady sequence of rain events for 15 days, and Event A4 only one previous day of intense rainfall. Although both events measured a similar rainfall intensity, the VR on Event A2 retained 35 % less rainwater.

This finding is relevant when implementing VRs in the subtropical climate, as during rainy or dryer seasons it can perform differently. Connecting back to the introduction of this work regarding subtropical specificities, this finding resonates to Hakimdavar et al. (2014), as not only the higher incidence of storm events in the tropics diminish the VR retention performance, but also one parameter that influences this phenomenon the most is the event duration. Very strong tropical storm events, thus, may influence the retention of a VR, but this influence should be much greater if these events are longer and under cloudy conditions, when evaporation and transpiration won't happen as much.

4. Conclusion

The combination of the two main novel findings of this work regarding subtropical climate and unmanaged vegetation can shed light to new opportunities for vegetated roofs in this particular climate. By letting the vegetation grow freely, the biomass will adapt to the available soil moisture content and thus to the available stormwater. Designing VRs with less substrate depth, but more vegetation and specially with native and spontaneous species and leaving it unmanaged can generate a lighter weight structure with a high retention rate and a low maintenance need. As maintenance in general is a burden for many green infrastructures, having a vegetated roof that can perform hydrologically well in subtropical conditions under low maintenance is a cost-effective solution provided by unmanaged roofs both in terms of less structure necessary to hold its weight and also less work needed for upkeep. Some level of maintenance, though, is suggested so that invasive or highly reproductive species won't dominate the vegetated roofs, as pointed out by Leite et al. (2022).

Further work to implement the aforementioned results into urban rainwater systems is needed in order to observe whether the positive outcomes are maintained or changed. The present work results are representative of summer periods in subtropical areas, a moment when solar radiation is higher, generating higher soil desaturation. But also, a moment when rainfall events are more intense and more frequent. To address this limitation and provide general results and recommendations, further work for winter periods is necessary and will be undertaken. Other relevant limitation in this work is the very narrow return period heterogeneity monitored, as the representative events were all under 2 years of return period, indicating the need to monitor longer return periods. On top of that, it is also difficult to guarantee a consistency between spontaneous species colonizing the VR. To better characterize the role of vegetation in changing the hydrological performance of unmanaged VR, would be interesting to monitor a larger number of identical models for each substrate depth in order to more realistically describe trends and average performances.

VRs can have a great urban impact towards a sustainable and decentralized drainage future. Along with its many benefits, many dwellers and architects are choosing green rooftops. But for a real impact on urban scales, VR should become a public policy and be largely adopted. For that to be possible, a standardization is necessary, which, including Brazil, many mainly tropical and subtropical countries still do not have. Towards a proper standardization, it is imperative not only to know qualitatively the VR performance, but also to quantify it and find cost-effective solutions. Hence, these results may contribute not only to the incorporation of VR in architectural projects, but also to an urban scale application, given that unmanaged VR can be less structurally demanding and less maintenance demanding.

CRediT authorship contribution statement

Lucas Gobatti: conceptualization, methodology, formal analysis, investigation, resources, data curation, visualization, funding acquisition and original draft writing. **Brenda Leite:** validation, resources, writing review, supervision, project administration and funding acquisition.

Data availability

Data is shared on Mendeley Data in the manuscript and is found in the reference list.

Declaration of competing interest

The authors declare that they have no known competing financial interests or personal relationships that could have appeared to influence the work reported in this paper.

Acknowledgements

This work was supported by the Santander Bank *via* USP Municipalities Notice 01/2021 “Desafio USP: cidades sustentáveis” [grant number 2021.1.471.3.0] and the São Paulo State Research Support Foundation (FAPESP) [grant number 2010/09149-9]. The funding sources provided financial support, but had no direct involvement in the research or publication of this work.

The authors acknowledge the material and technical support from Forseti Soluções and the Foundation Hydraulics Technological Center (FCTH) in the figure of Prof. Rodolfo Scarati and Eng. Maria Cristina Santana Pereira. The authors also thank Prof. Sally Elizabeth Thompson for the valuable suggestions to this manuscript, Prof. Fábio Lofrano for contributing in the research discussion on unsaturated soil mechanics and the illustrator Henrique Capanema for contributing with Fig. 1. Full research data is available in Mendeley Data (Database).

Appendix A. Supplementary data

Supplementary data to this article can be found online at https://doi.org/10.1016/j.scitotenv.2023.162417.

References

Aloisio, J.M., Palmer, M.I., Tuininga, A.R., Lewis, J.D., 2020. Introduced and native plant species composition of vacant unmanaged green roofs in New York City. Urban Ecosyst. 23, 1227–1238. https://doi.org/10.1007/s11252-020-00992-6.

Alvares, C.A., Stape, J.L., Sentelhas, P.C., Gonçalves, J.L.M., Sparovek, G., 2014. Köppen's climate classification map for Brazil. Meteorol. Z. 22 (6), 711–728. https://doi.org/10.1127/0941-2948/2013/0507.

Arboit, N.K.S., Tassi, R., Liberalesso, T., Ceconi, D.E., Piccili, D.G.A., 2021. Green roof evapotranspiration rates and stormwater control under subtropical climate: a case study in Brazil. Brazilian Journal of Water Resources 26, e32. https://doi.org/10.1590/2318-0331.262120210089 ISSN 2318-0331.

Baptista, M.B., Nascimento, N.O., Barraud, S., 2011. Técnicas compensatórias em drenagem urbana. ABRH, Porto Alegre, RS, Brazil 978-85-8868-631-1.

Berndtsson, J.C., 2010. Green roof performance towards management of runoff water quantity and quality: a review. Ecol. Eng. 36 (4), 351–360. https://doi.org/10.1016/j.ecoleng.2009.12.014.

Blank, L., Vasl, A., Levy, S., Grant, G., Kadas, G., Dafni, A., Blaustein, L., 2013. Directions in green roof research: a bibliometric study. Build. Environ. 66, 23–28. https://doi.org/10.1016/j.buildenv.2013.04.017 ISSN 0360–1323.

Castillo, R.M., Crisman, T.L., 2019. The Role of Green Infrastructure in Water, Energy and Food Security in Latin America and the Caribbean: Experiences, Opportunities and Challenges. Inter-American Development Bank https://doi.org/10.18235/0001920.

Castro, A.S., Goldenfum, J.A., da Silveira, A.L., et al., 2020. The analysis of green roof's runoff volumes and its water quality in an experimental study in Porto Alegre, southern Brazil. Environ. Sci. Pollut. Res. 27, 9520–9534. https://doi.org/10.1007/s11356-019-06777-5.

Catalano, C., Marcenò, C., Laudicina, V.A., Guarino, R., 2016. Thirty years unmanaged green roofs: Ecological research and design implications. Landscape and Urban Planning 149 (May 2016), 11–19. https://doi.org/10.1016/j.landurbplan.2016.01.003.

Cook-Patton, S.C., Bauerle, T.L., 2012. Potential benefits of plant diversity on vegetated roofs: a literature review. J Environ Manage 106 (2012 Sep 15), 85–92. https://doi.org/10.1016/j.jenvman.2012.04.003.

DAEE-CTH, 2018. Precipitações intensas do Estado de São Paulo (Intense precipitations of São Paulo State, Brazil). . Available at. http://www.daee.sp.gov.br/site/hidrologia/. (Accessed 23 May 2022).

Davis Instruments, 2021. Vantage Vue weather station specification sheet. Available at https://www.davisinstruments.com/products/vantage-vue-wireless-weather-station.

Demirkesen, A.C., 2001. Constructing a prior information base for river mapping from digital images and dems by an advanced image interpretation system. Thesis (PhD)Ohio State University Publication Number: AAI3022472; ISBN: 9780493340173.

Deng, H., Jim, C.Y., 2017. Spontaneous plant colonization and bird visits of tropical extensive green roof. Urban Ecosyst. 20, 337–352. https://doi.org/10.1007/s11252-016-0596-3.

Deng, J.S., Wang, K., Hong, Y., Qi, J.G., 2009. Spatio-temporal dynamics and evolution of land use change and landscape pattern in response to rapid urbanization. Landsc. Urban Plan. 92 (3–4), 187–198. https://doi.org/10.1016/j.landurbplan.2009.05.001.

Dierkes, C., Lucke, T., Helmreich, B., 2015. General technical approvals for decentralised sustainable urban drainage systems (SUDS)—the current situation in Germany. Sustainability. 7 (3), 3031–3051. https://doi.org/10.3390/su7033031.

Dunnett, N., Kingsbury, N., 2014. Planting Green Roofs and Living Walls. Timber Press, Portland.

Dunnett, N., Nagase, A., Hallam, A., 2008. The dynamics of planted and colonising species on a green roof over six growing seasons 2001–2006: influence of substrate depth. Urban Ecosyst. 11, 373–384. https://doi.org/10.1007/s11252-007-0042-7.

El Hattab, M.H., Mijic, A., Vernon, D., 2018. Optimised triangular weir design for assessing the full-scale performance of green infrastructure. Water 11 (4), 773. https://doi.org/10.3390/w11040773.

Extech, 2009. Datasheet MO290-EP extension probes. Available at: http://www.extech.com/products/resources/MO290-xx_DS-en.pdf.

Extech, 2014. Pinless Moisture/Humidity meter with IR thermometer + bluetooth user guide. Available at: http://www.extech.com/products/resources/MO297_UM-en.pdf.

Ferrans, P., Rey, C.V., Pérez, G., Rodríguez, J.P., Díaz-Granados, M., 2018. Effect of green roof configuration and hydrological variables on runoff water quantity and quality. Water 10 (7), 960. https://doi.org/10.3390/w10070960.

Ferraz, I.L., 2012. The thermal performance of green roof system in comparison to the traditional ceramic tile roof system. University of São Paulo, SP, Brazil https://doi.org/10.11606/D.3.2012.tde-07062013-144209 Thesis (Masters).

Garofalo, G., Palermo, S., Principato, F., Theodosiou, T., Piro, P., 2016. The influence of hydrologic parameters on the hydraulic efficiency of an extensive green roof in Mediterranean area. Water. 8 (2), 44. https://doi.org/10.3390/w8020044.

Getter, K.L., Bradley Rowe, B.D., Cregg, B.M., 2009. Solar radiation intensity influences extensive green roof plant communities. Urban Forestry & Urban Greening 8 (4), 269–281. https://doi.org/10.1016/j.ufug.2009.06.005 ISSN 1618-8667.

Gobatti, L., Leite, B.C.C., 2022. Vegetated roofs rainwater management experimental research in Brazil: a georeferenced exhaustive review of a continental-size country. Clean. Prod. Lett. 3. https://doi.org/10.1016/j.clpl.2022.100013.

Gobatti, L., Leite, B.C.C., 2022]. Ten years unmanaged extensive green roofs and the effects of substrate depth: a comparative water quantity performance investigation in Brazil. [Database]Mendeley Data (V2) Doi:10.17632/p942b9vkhs.2.

Gobatti, L., Martins, J.R.S., Pereira, M.C.S., Leite, B.C.C., 2022. Real-time sensing and low-cost experimental setup for water quantity investigation in nature-based solutions. Blue-Green Systems 4 (2). https://doi.org/10.2166/bgs.2022.007.

Grullón-Penkova, I.F., Zimmerman, J.K., González, G., 2020. Green roofs in the tropics: design considerations and vegetation dynamics. Heliyon 6, e04712. https://doi.org/10.1016/j.heliyon.2020.e04712.

Hakimdavar, R., Culligan, P.J., Finazzi, M., Barontini, S., Ranzi, R., 2014. Scale dynamics of extensive green roofs: quantifying the effect of drainage area and rainfall characteristics on observed and modeled green roof hydrologic performance. Ecol. Eng. 73, 494–508. https://doi.org/10.1016/j.ecoleng.2014.09.080 ISSN 0925–8574.

Han, S., Burian, S.J., 2009. Determining effective impervious area for urban hydrologic modeling. J. Hydrol. Eng. 14 (2), 111–120. https://doi.org/10.1061/(ASCE)1084-0699(2009)14:2(111).

Hill, J., Perotto, M., Yoon, C., 2015. Quantifying the hydrological performance of extensive vegetative roofs. Available at30th RCI International Convention and Trade Show . https://citeseerx.ist.psu.edu/viewdoc/download?doi=10.1.1.724.7185&rep=rep1&type=pdf.

Jacobson, C.R., 2011. Identification and quantification of the hydrological impacts of imperviousness in urban catchments: a review. J. Environ. Manag. 92 (6), 1438–1448. https://doi.org/10.1016/j.jenvman.2011.01.018.

Johannessen, B.G., Muthanna, T.M., Braskerud, B.C., 2018. Detention and retention behavior of four extensive green roofs in three nordic climate zones. Water. 10 (6), 671. https://doi.org/10.3390/w10060671.

Krauze, K., Wagner, I., 2019. From classical water-ecosystem theories to nature-based solutions — contextualizing nature-based solutions for sustainable city. Sci. Total Environ. 655, 697–706. https://doi.org/10.1016/j.scitotenv.2018.11.187 ISSN 0048–9697.

Leite, B.C.C., Gobatti, L., Huttenlocher, I.G., 2022. Low-maintenance subtropical green roofs: spontaneous vegetation and substrate depth. AGATHÓN, n. 11, 258–265. https://doi.org/10.19229/2464-9309/11232022.

Liberalesso, T., Tassi, R., Ceconi, D.E., Allasia, D.G., Arboit, N.K.S., 2021. Effect of rice husk addition on the physicochemical and hydrological properties on green roof substrates under subtropical climate conditions. J. Clean. Prod. 315. https://doi.org/10.1016/j.jclepro.2021.128133.

Liu, W., Feng, Q., Chen, W., Wei, W., Deo, R.C., 2019. The influence of structural factors on stormwater runoff retention of extensive green roofs: new evidence from scale-based models and real experiments. J. Hydrol. 569, 230–238. https://doi.org/10.1016/j.jhydrol.2018.11.066 ISSN 0022–1694.

Liu, H., Kong, F., Yin, H., Middel, A., Zheng, X., Huang, J., Xu, H., Wang, D., Wen, Z., 2021. Impacts of green roofs on water, temperature, and air quality: a bibliometric review. Build. Environ. 196, 107794. https://doi.org/10.1016/j.buildenv.2021.107794 ISSN 0360–1323.

Locatelli, L., Mark, O., Mikkelsen, P.S., Arnbjerg-Nielsen, K., Jensen, M.B., Binning, P.J., 2014. Modelling of green roof hydrological performance for urban drainage applications. Journal of Hydrology 519 (Part D), 3237–3248. https://doi.org/10.1016/j.jhydrol.2014.10.030 ISSN 0022-1694.

Loiola, C., Mary, W., Silva, L.P., 2019. Hydrological performance of modular-tray green roof systems for increasing the resilience of mega-cities to climate change. J. Hydrol. 573, 1057–1066. https://doi.org/10.1016/j.jhydrol.2018.01.004 ISSN 0022–1694.

Madre, F., Vergnes, A., Machon, N., Clergeau, P., 2014. Green roofs as habitats for wild plant species in urban landscapes: First insights from a large-scale sampling. Landscape and Urban Planning 122 (February 2014), 100–107. https://doi.org/10.1016/j.landurbplan.2013.11.012.

Martinelli, M., 2010. Clima do Estado de São Paulo (Climate of São Paulo State). 8. Revue Franco-Brésilienne de Géographie. https://doi.org/10.4000/confins.6348.

Miguez, M.G., Veról, A.P., De Sousa, M.M., Rezende, O.M., 2015. Urban floods in lowlands—Levee systems, unplanned urban growth and river restoration alternative: a case study in Brazil. Sustainability 7 (8), 11068–11097. https://doi.org/10.3390/su70811068.

Nair, S.K.A., Joladarashi, S., Ganesh, N., 2019. Proceedings of the Third International Conference on Trends in Electronics and Informatics (ICOEI 2019), pp. 638–641 https://doi.org/10.1109/ICOEI.2019.8862659.

Naveen, H., Narasimhan, S., George, B., Tangirala, A.K., 2020. Design and development of a low-cost cantilever-based flow sensor. IFAC-PapersOnLine 53 (1), 111–116. https://doi.org/10.1016/j.ifacol.2020.06.019.

Oberndorfer, E., Lundholm, J., Bass, B., Coffman, R.R., Doshi, H., Dunnett, N., Gaffin, S., Köhler, M., Liu, K.K.Y., Rowe, B., 2007. Green roofs as urban ecosystems: ecological structures, functions, and services. Bioscience 57 (10), 823–833. https://doi.org/10.1641/B571005.

Onset, 2022. S-LIB-M003 Solar Radiation (Silicon Pyranometer) Smart Sensor Datasheet. Available at. https://www.onsetcomp.com/datasheet/S-LIB-M003.

Onset, 2022. HOBO H21-USB data logger USB Micro Station datasheet. Available at: https://www.onsetcomp.com/datasheet/H21-USB.

Ouellet, V., Khamis, K., Croghan, D., Hernandez Gonzalez, Rivera, V.A., Phillips, C.B., Packman, A.I., Miller, W.M., Hawke, R.G., Hannah, D.M., Krause, S., 2021. Green roof vegetation management alters potential for water quality and temperature mitigation. Ecohydrology 14 (6), e2321.. https://doi.org/10.1002/eco.2321.

Panda, K.G., Agrawal, D., Nshimiyimana, A., Hossain, A., 2016. Effects of environment on accuracy of ultrasonic sensor operates in millimetre range. perspectivesScience 8, 574–576. https://doi.org/10.1016/j.pisc.2016.06.024 ISSN 2213–0209.

Péné, C.B., N'Diaye, S., N'Guessan-Konan, C., 2021. Study on sprinkler irrigation and soil tillage practices in sugarcane plantations as influenced by soil texture and water storage in northern Ivory Coast. Current Topics in Agricultural Sciences. 1, pp. 1–9. https://doi.org/10.9734/bpi/ctas/v1/11583D.

Peng, Z., Smith, C., Stovin, V., 2019. Internal fluctuations in green roof substrate moisture content during storm events: Monitored data and model simulations. Journal of Hydrology 573, 872–884. https://doi.org/10.1016/j.jhydrol.2019.04.008 ISSN 0022-1694.

Persch, C.G., Tassi, R., Minetto, B., Allasia, D.G., 2021. Assessing the scale dynamics of the rainfall retention of green roofs in a subtropical climate. J. Environ. Eng. 147 (11), 04021054. https://doi.org/10.1061/(ASCE)EE.1943-7870.0001933.

Poë, S., Stovin, V., Berretta, C., 2015. Parameters influencing the regeneration of a green roof's retention capacity via evapotranspiration. Journal of Hydrology 523 (2015), 356–367. https://doi.org/10.1016/j.jhydrol.2015.02.002 ISSN 0022-1694.

Rain Bird, 2003. Creating Beautiful Landscapes is Easy With Rain Bird Drip Products. Azusa, CA. Available at. https://www.rainbird.com.br/upload/ferramentas-de-trabalho/Manuais-Xerigation/DripDesignGuide.pdf.

Robinson, S.L., Lundholm, J.T., 2012. Ecosystem services provided by urban spontaneous vegetation. Urban Ecosyst 15, 545–557.. https://doi.org/10.1007/s11252-012-0225-8.

Schrieke, D., Farrell, C., 2021. Trait-based green roof plant selection: water use and drought response of nine common spontaneous plants. Urban Forestry & Urban Greening 65 (November 2021), 127368. https://doi.org/10.1016/j.ufug.2021.127368.

Shafique, M., Kim, R., Rafiq, M., 2018. Green roof benefits, opportunities and challenges – a review. Renew. Sust. Energ. Rev. 90, 757–773. https://doi.org/10.1016/j.rser.2018.04.006 ISSN 1364–0321.

Shen, J., 1981. Discharge characteristics of triangular-notch thin-plate weirs: studies of flow of water over weirs and dams. Available atGeological Survey Water-supply Paper 1617-B. United States Government Printing Office, Washington . https://pubs.usgs.gov/wsp/1617b/report.pdf.

Shuster, W.D., Bonta, J., Thurston, H., Warnemuende, E., Smith, D.R., 2007. Impacts of impervious surface on watershed hydrology: a review. Urban Water J. 2 (4), 263–275. https://doi.org/10.1080/15730620500386529.

Silva, C.M., Flores-Colen, I., Antunes, M., 2017. Step-by-step approach to ranking green roof retrofit potential in urban areas: a case study of Lisbon, Portugal. Urban For. Urban Green. 25, 120–129. https://doi.org/10.1016/j.ufug.2017.04.018 ISSN 1618–8667.

Soulis, K.X., Ntoulas, N., Nektarios, P.A., Kargas, G., 2017. Runoff reduction from extensive green roofs having different substrate depth and plant cover. Ecol. Eng. 102, 80–89. https://doi.org/10.1016/j.ecoleng.2017.01.031.

Stevaux, J.C., Latrubesse, E.M., Hermann, M.L.P., Aquino, S., 2009. Floods in urban areas of Brazil. In: Latrubesse, Edgardo M. (Ed.), Developments in Earth Surface Processes. 13. Elsevier, pp. 245–266. https://doi.org/10.1016/S0928-2025(08)10013-X ISSN 0928-2025, ISBN 9780444531179.

Stovin, V., 2010. The potential of green roofs to manage urban stormwater. Water Environ. J. 24, 192–199. https://doi.org/10.1111/j.1747-6593.2009.00174.x.
Tellinghuisen, J., 2001. Statistical error propagation. J. Phys. Chem. A 105 (15), 3917–3921. https://doi.org/10.1021/jp003484u.
Thuring, C.E., Dunnett, N.P., 2019. Persistence, loss and gain: characterising mature green roof vegetation by functional composition. Landscape and Urban Planning 185 (May 2019), 228–236. https://doi.org/10.1016/j.landurbplan.2018.10.026.
Tucci, C.E.M., 2005. Modelos Hidrológicos (Hydrological Models). 2nd ed. ABRH and Editora UFRGS, Porto Alegre.
Vacari, T.C., Lara, J.R., Lima, Z.M.L., Morais, E.B., 2019. Water quantity investigation of simulated green roofs in a tropical climate: influence of vegetation composition. ES Eng. Sci. 8 (2), 2–14. https://doi.org/10.18607/ES201988046.
Vanstockem, J., Somers, B., Hermy, M., 2019. Weeds and gaps on extensive green roofs: ecological insights and recommendations for design and maintenance. Urban For. Urban Green. 46. https://doi.org/10.1016/j.ufug.2019.126484.
VanWoert, N.D., Rowe, D.B., Andresen, J.A., Rugh, C.L., Fernandez, R.T., Xiao, L., 2005. Green roof stormwater retention. J. Environ. Qual. 34, 1036–1044. https://doi.org/10.2134/jeq2004.0364.
Vesuviano, G., Stovin, V., 2013. A generic hydrological model for a green roof drainage layer. Water Sci. Technol. 68 (4), 769–775. https://doi.org/10.2166/wst.2013.294.
Vörösmarty, C.J., Bravo, G.L., Wollheim, W.M., Pellerin, B., Bjerklie, D., Cardoso, M., D'Almeida, C., Green, P., Colon, L., 2013. Extreme rainfall, vulnerability and risk: a continental-scale assessment for South America. Phil. Trans. R. Soc. https://doi.org/10.1098/rsta.2012.0408.
Voyde, E., Fassman, E., Simcock, R., 2010. Hydrology of an extensive living roof under subtropical climate conditions in Auckland, New Zealand. J. Hydrol. 394 (3–4), 384–395. https://doi.org/10.1016/j.jhydrol.2010.09.013 ISSN 0022–1694.
Wang, Y., Zhang, X., Xu, J., Pan, G., Zhao, Y., Liu, Y., Liu, H., Liu, J., 2022. Accumulated impacts of imperviousness on surface and subsurface hydrology—continuous modelling at urban street block scale. Journal of Hydrology 608, 127621. https://doi.org/10.1016/j.jhydrol.2022.127621 ISSN 0022-1694.